THE V-R3X MISSION: TOWARDS AUTONOMOUS NETWORKING AND NAVIGATION FOR CUBESAT SWARMS

Max Holliday[1], **Kevin Tracy**[2], **Zachary Manchester**[3], **and Anh Nguyen**[4]

[1]*Stanford University, 496 Lomita Mall, Stanford, CA 94305 USA, maholli@stanford.edu*
[2]*Carnegie Mellon University, 5000 Forbes Ave. Pittsburgh, PA 15213 USA, ktracy@cmu.edu*
[3]*Carnegie Mellon University, 5000 Forbes Ave. Pittsburgh, PA 15213 USA, zacm@cmu.edu*
[4]*NASA Ames Research Center, Mailstop N202-3, Moffett Field, CA 94035 USA, anh.n.nguyen@nasa.gov*

Abstract

The V-R3x project aims to enable autonomous swarms of small spacecraft by both reducing the manufacturing cost and integration effort required for each individual spacecraft, and by developing advanced radio communication and navigation capabilities that reduce or eliminate reliance on Earth-based navigation infrastructure like GPS. To achieve these goals, a low-cost CubeSat avionics and flight software stack that is capable of high-data-rate radio cross linking and precise two-way time-of-flight ranging between spacecraft has been developed, as well as navigation algorithms that can estimate relative and absolute orbital positions by fusing inter-satellite range measurements with GPS or other navigation measurements. These capabilities have been demonstrated on terrestrial, high-altitude balloon, and on-orbit test campaigns over the past year.

1. INTRODUCTION

The advent of CubeSats and availability of low-cost commercial ride-share services have increased interest in missions involving formations or swarms of multiple spacecraft. Such mission concepts offer the promise of continuous coverage of the Earth for observation and communication services [1]–[3], large baselines for high-resolution radio and optical astronomy [4], [5], and distributed in-situ measurements of the ionosphere and solar wind [6], [7]. However, current methods for performing the basic relative navigation functions required for multi-spacecraft swarms involve some combination of expensive, specialized hardware; highly centralized coordination and control, typically performed by ground operators; and limited ability to function beyond low-Earth orbit due to reliance on GPS or other Global Navigation Satellite System (GNSS) signals.

The V-R3x project aims to develop and demonstrate low-cost sensing, communication, and navigation capabilities to enable scalable, autonomous CubeSat swarms. This includes building on a highly integrated open-source avionics stack that relies on commercial off-the-shelf (COTS) electronic components to reduce manufacturing costs, and developing novel navigation algorithms that can be implemented in flight software onboard compute-constrained CubeSats. V-R3x is a collaboration between researchers at Stanford University, Carnegie Mellon University, and NASA Ames Research Center, and is based on the open-source PyCubed avionics and software platform [8].

To reduce hardware costs to an absolute minimum, V-R3x makes use of COTS LoRa radio modules that perform both communication and two-way time-of-flight ranging between spacecraft [9]. These range measurements are fused with orbital dynamics models and other navigation measurements — such as occasional GPS measurements from a single satellite or ground-based measurements — using novel state-estimation algorithms to determine the full orbital parameters of the entire swarm. To date, these systems have been tested in both high-altitude balloon flights and in an orbital demonstration involving three 1U CubeSats, with additional future orbital experiments planned.

The paper proceeds as follows: Section 2 provides an an overview of the V-R3x mission concept, followed by a discussion of the spacecraft's hardware, electronic, and software design in Section 3. Section 4 then provides a derivation and analysis of the range-based relative-navigation algorithms developed for V-R3x. Section 5 describes a sub-orbital and orbital test campaign that was undertaken in 2021 to evaluate the performance of both the hardware and software components of V-R3x. Finally, Section 6 summarizes our conclusions, lessons learned, and directions for future work.

2. MISSION CONCEPT

The V-R3x mission is designed to demonstrate radio cross linking, networking, and relative navigation between low-cost CubeSats. The mission includes three 1U CubeSats, to be deployed together into a roughly 500 km altitude circular, sun-synchronous orbit. A summary of spacecraft operations is illustrated in Fig. 1.

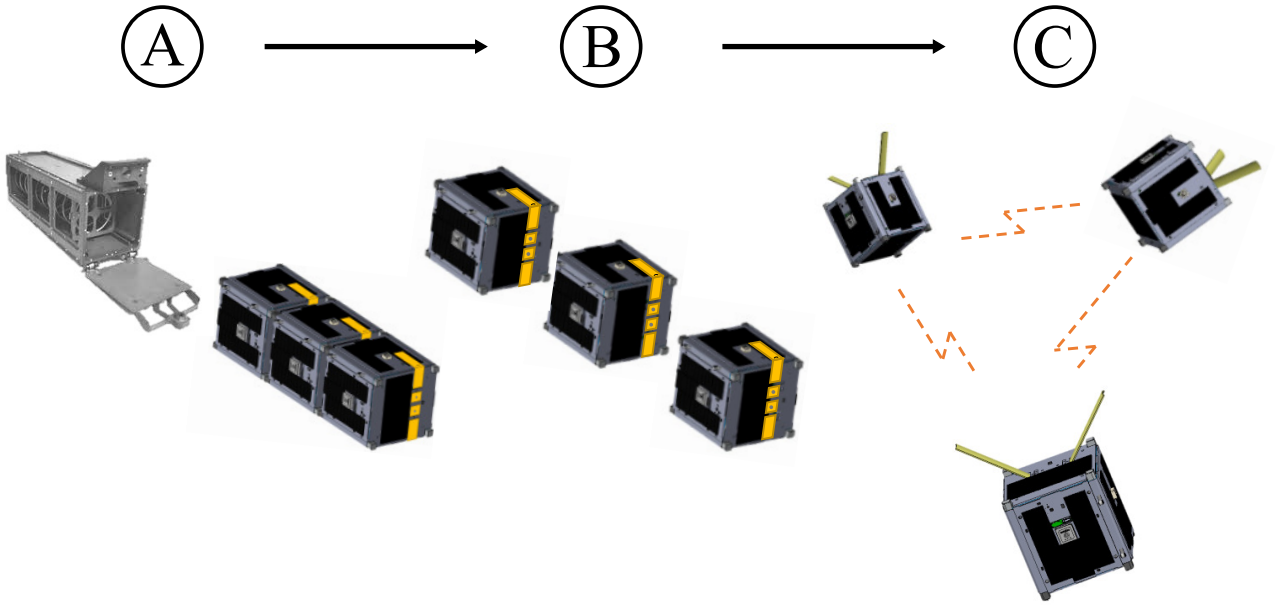

Figure 1. The V-R3x mission timeline. From left to right: (A) Spacecraft are ejected from their dispenser. (B) Spacecraft slowly separate. (C) Spacecraft perform nominal operations, including networking and two-way time-of-flight ranging with radio crosslinks.

The three V-R3x spacecraft are expected to exit their dispenser in a slow tumble with small initial relative linear and angular velocities. Since they do not have propulsion or attitude control systems, the spacecraft are expected to drift apart over time due to both their initial relative velocities and the integrated effects of differential drag. Extensive Monte-Carlo simulations with a range of possible atmospheric conditions and realistic initial velocities at deployment bound the drift rate between spacecraft between approximately 0.9 and 2.5 kilometers per hour. The spacecraft are expected to drift out of range of each other a few weeks after deployment.

To ensure that networking and ranging between all three spacecraft can be accomplished across different distances, the spacecraft are designed to begin transmitting immediately after deployment and to perform ranging and networking experiments continuously using their 2.4 GHz LoRa radios. All data will be logged to non-volatile memory onboard the spacecraft to be downlinked later. Constant use of their radios puts the spacecraft in a power-negative state that will deplete their batteries. The flight software is written such that the spacecraft will enter a low-power mode, which will stop radio experiments, if the battery voltage drops below a critical threshold. Alternatively, a command from a ground station can also be used to put the spacecraft into a low-power mode.

Simultaneously with ranging and networking experiments, the three V-R3x spacecraft will collect GPS position and velocity data to provide precision timestamps for all experimental data and to provide ground-truth positions to validate LoRa range measurements. Since individual GPS position measurements are less accurate than the range measurements from the LoRa radios, GPS data will be filtered in post-processing using standard Kalman smoother techniques to produce more accurate position estimates.

In addition to navigation experiments, each V-R3x spacecraft will also collect total-ionizing dose (TID) radiation measurements once every 30 seconds with the intent of creating dense temporal and spatial dose-rate datasets. Custom dosimeters that will be used to collect this TID information are comprised of the threshold voltage (V_{TH}) direct readout circuit described in [10] for monitoring V_{TH} shifts in a commercial P-channel MOSFET (Vardis VT01) designed for dosimetry with known TID response characteristics.

All three V-R3x spacecraft transmit a beacon message every 30 seconds using their 915 MHz UHF LoRa radios. Each beacon is a single packet with a 45-byte payload containing state-of-health information, mission status, and a revolving

summary of navigation and radiation experiment data. Command and control of the spacecraft is achieved by uplinking commands to the spacecraft during a 10-second window following each beacon transmission.

Once the primary data-collection phase of the mission is completed — likely within the first two weeks of the mission depending on the drift rates between the spacecraft — all of the data stored on the three spacecraft will be downlinked opportunistically to ground stations. This is accomplished by uplinking a single command to one of the spacecraft to place it into data downlink mode, at which point all stored experimental data is transmitted at a high data rate by the UHF LoRa radio. Given the expected data volume from the mission, all data accumulated by a single spacecraft should be transferable to a ground station within a few minutes — well within the time of a typical ground station pass.

After all data is downlinked from the three V-R3x spacecraft, the primary mission will be complete. While the spacecraft will drift out of range of each other and will no longer be able to perform inter-satellite communication or ranging, they may still be used for additional communication and navigation experiments with ground stations. The top-level requirements for the V-R3x mission are summarized in Table 1.

Table 1. V-R3x Primary Mission Requirements

Requirement	**Description**
S-Band Crosslink	V-R3x shall demonstrate data rates >50 Kbps (up to 250 kbps) between two satellite nodes at distances up to 10 km between at least two satellite nodes.
S-Band Precision Ranging	V-R3x shall demonstrate ranging with <1 m precision at distances up to 500 km between at least two satellite nodes.
Relative Navigation	V-R3x shall demonstrate relative positioning between all satellite nodes (post processed on the ground).
Distributed Sensor Collection	V-R3x shall coordinate and collect radiation data from on-board sensors from each satellite node.

3. SPACECRAFT DESIGN

The V-R3x spacecraft were developed with minimizing hardware cost and development time as primary drivers. All aspects of the spacecraft were developed in-house by a small team from conception to launch in less than one year, including:

- avionics systems: power handling, energy harvesting, data processing, sensors, and data storage
- low-level firmware
- flight software: mesh networking scheme, S-band ranging, ground communication, and over-the-air updating
- mechanical design
- hardware fabrication and electronics assembly
- flight hardware fabrication and assembly

This extremely fast development time was enabled by the use of open-source avionics and software from the PyCubed project [8], which has been developed by the authors over several years. A cutaway illustration depicting the primary subsystems of the 1U V-R3x CubeSat is shown in Fig. 2. These subsystems are detailed in the following subsections.

3.1. Mechanical

V-R3x is built to conform to the 1U CubeSat specification. Each spacecraft's mass is approximately 1 kg. The spacecraft structures are standard 1U anodized aluminum chassis from Pumpkin, Inc. with minor modifications to accommodate antenna, solar panel, and deployment switch mounting hardware. The UHF dipole antenna is made from steel spring tape and is designed to be folded against the exterior faces of the CubeSat when mounted in the dispenser. A waiver was obtained for V-R3x to allow its dipole antenna to be left unsecured in the dispenser (i.e. a burn wire deployment mechanism was not employed). This was done to eliminate risk and enable activation of the spacecraft's cross-link radios immediately after deployment. The three fully assembled 1U flight units are pictured in Fig. 3.

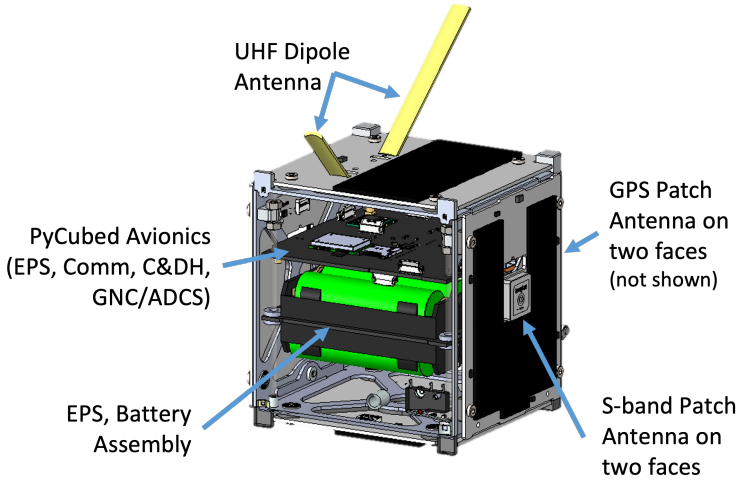

Figure 2. Cutaway view of the V-R3x spacecraft showing the locations of avionics, batteries, and antennas.

Figure 3. All three fully assembled V-R3x flights unit in deployed configuration. Note the presence of a UHF dipole antennas on the +Z face of the spacecraft, GPS patch antennas on the +/-X faces of the spacecraft, and S-band patch antennas on the +/-Y faces of the spacecraft.

3.2. Energy Harvesting and Power Regulation

On-orbit energy harvesting is performed by the PyCubed solar maximum power-point tracking (MPPT) circuit supplied by custom spacecraft solar panels built from low-cost COTS solar cells (part number: SM141K06L). Based around the Analog Devices LTC4121 chip, the MPPT circuit was configured for a target voltage of 75% of the open circuit panel voltage (V_{OC}) with a maximum charge rate of 400 mA.

Spacecraft power regulation relies on the PyCubed on-board DC-DC converter (part number: TPS54226PWPR) to efficiently regulate the 2S3P (8.4 V) battery voltage to provide 3.3 V necessary to power various spacecraft subsystems. The decision to use the TPS542XX family of DC-DC converters from Texas Instruments was based on its radiation performance, regulator efficiency, and configurable output voltage. Having been evaluated for TID and SEE tolerance by multiple researchers [11], Cochran et al. reported a TID tolerance of 15 to 20 krad [12], and Allen et al. reported no destructive SEL events occurring on devices biased at 10V or less and under a variety of temperature conditions [13].

3.3. Communication, Sensing, and Navigation

Cross-link communication and two-way time-of-flight ranging are both provided by Semtech SX1280 (S-band) LoRa radio modules. These radios have a transmit power of 0.5 W and utilize the unique LoRa chirp spread-spectrum modulation. Due to their large bandwidth, LoRa chirp signals are ideal for performing accurate range measurements between two radios. While this sort of time-of-flight ranging has been implemented in software with previous LoRa radios, the SX1280 is the first LoRa module to implement ranging capabilities at the hardware level. As a result, sub-meter range accuracy is achievable with careful calibration [9]. With a cost of only a few dollars, the SX1280 provides a very low-cost relative-navigation solution for CubeSats.

In addition to the S-band SX1280 radio, the V-R3x spacecraft also carry a UHF LoRa radio (Semtech SX1276) for communication with ground stations. This radio module has an output power of 1W and is optimized for extremely robust communication at low data rates for telemetry, tracking, and command. A high-data-rate mode for this radio is also implemented in flight software for downlinking large volumes of experimental data at the end of the primary mission.

To provide ground-truth navigation data to validate LoRa range measurements, the V-R3x spacecraft are also equipped with GPS receivers. Skytraq S1216 modules with COCOM limits removed were integrated onto the PyCubed mainboard and connected to a pair of external patch antennas through an RF splitter-combiner to minimize periodic fading due to tumbling. In addition to GPS, the spacecraft are also equipped with inertial measurement units (part number: LSM9DS1) to collect angular velocity measurements.

Finally, each V-R3x spacecraft is also equipped with a custom-built radiation dosimeter to collect total ionizing dose (TID) information. These sensors work by measuring the threshold voltage (V_{TH}) in a commercial P-channel MOSFET designed for dosimetry with known TID response characteristics (part number: Vardis VT01). A custom direct-readout circuit was developed to make these measurements [14].

3.4. Computing

The V-R3x spacecraft rely on a Microchip ATSAMD51 ARM Cortex M4F microcontroller as the primary flight computer. This 32-bit microcontroller is clocked at 120 MHz, has 192 kB of RAM and 512 kB of on-board flash memory, and has a hardware floating-point unit. External magnetic random access (MRAM) non-volatile flash memory (part number: MR25H40MDF) is used to store flight software in the form of plain-text Python source-code files and an external SD card (part number: SDSDQED-008G-XI) is used for data storage.

The ATSAMD51 microcontroller utilizes common serial communication protocols such as Inter-Integrated Circuit (I^2C) and Serial Peripheral Interface (SPI) to interface with the various on-board sensors, radios, and data storage devices. Including power monitors, sun sensors, and H-bridge drivers, a single V-R3x spacecraft can have up to 30 devices on a single I^2C bus. Given the inherent single-point failure mode of these serial protocols, an autonomous fault isolation circuit was developed [14]. By automatically isolating failed devices, the integrity of the bus is preserved without requiring additional signals or processing overhead from the host controller.

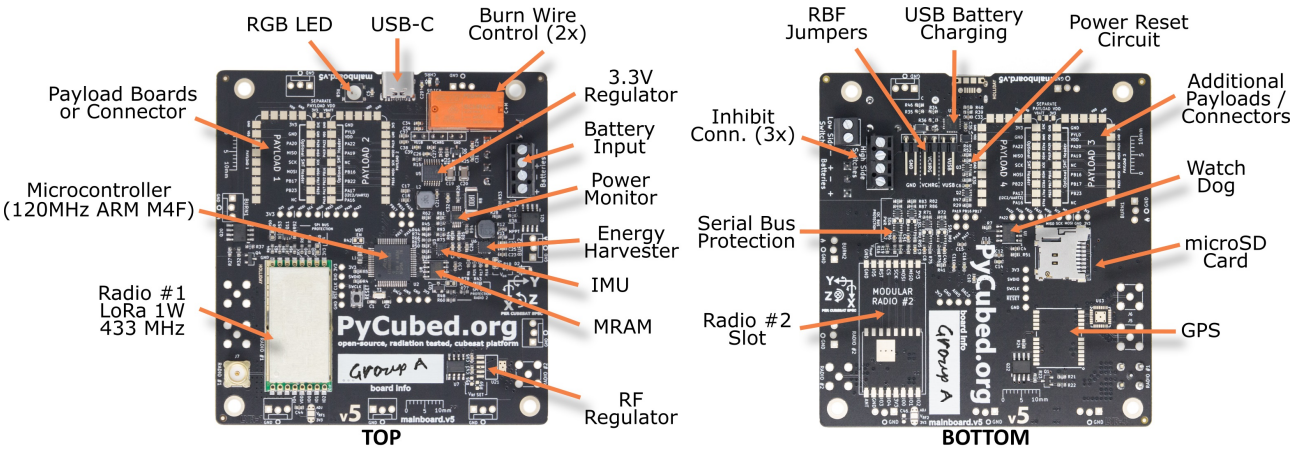

Figure 4. PyCubed mainboard. This single PC-104 board provides computing, power regulation, radio communication, GPS, and IMU capabilities. A very high level of integration reduces the overall size, weight, and cost of the spacecraft.

3.5. Flight Software

All high-level flight software executed on the V-R3x spacecraft is implemented in Python. As discussed in [8], the Micropython and CircuitPython real-time Python interpreters provide a robust CubeSat software architecture that is easy to learn, faster to program, and simpler to troubleshoot and debug than traditional embedded C and C++ approaches. The inherent compartmentalization, memory safety, and robust fault tolerance of Python's virtual machine enabled the rapid software development necessary for the V-R3x mission.

4. NAVIGATION ALGORITHMS

The V-R3x spacecraft use a combination of S-band inter-satellite ranging and GPS to perform full orbit determination. This section will use the target-chaser nomenclature, in which one spacecraft is arbitrarily labeled the "target" and the other two spacecraft are referred to as "chasers." For orbit determination and relative navigation, the target spacecraft is assumed to have access to full GPS position and velocity measurements, while the chaser spacecraft only have access to inter-satellite range measurements between the spacecraft. Since the ranging measurements are scalar distances, reconstructing the relative positions of the chaser spacecraft from the target is impossible given only a single measurement. In order to solve the orbit-determination problem for the two chaser spacecraft, a batch state-estimation problem is posed to reconstruct the position and velocity of the chaser spacecraft by combining GPS measurements from only the target with ranging measurements between all three spacecraft.

Traditionally, recursive Bayesian state-estimation techniques like the Kalman Filter [15] and its nonlinear extensions, including the Extended Kalman Filter [16], are highly capable methods for recovering full state estimates given limited sensing. However, in situations where the dynamics are highly nonlinear and the sensing is severely limited, a batch state estimation technique can perform better. Batch methods formulate the state estimation problem as an optimization problem that recovers the maximum *a-posteriori* probability (MAP) estimate of the state history given a history of measurements.

In order to formulate the orbit determination problem in this framework, first the dynamics function for the three spacecraft is defined:

$$x_{k+1} = f(x_k, \Delta t) + w_k. \tag{1}$$

Here, $f(x)$ is a nonlinear orbit propagator that takes the states of the three spacecraft at time k and propagates the orbits for one time step with high-order gravity and environmental perturbations. We assume Additive White Gaussian Noise (AWGN) $w_k \sim \mathcal{N}(0, Q)$ applied to the dynamics. This may not be the true nature of the disturbances, but modeling the uncertainty in the dynamics function as a Gaussian is often effective in practice. As for the measurement model, the estimator has access to the full GPS position and velocity measurement from the target spacecraft, as well as the three scalar ranges between the satellites. These measurements are described by the following measurement function:

$$y_k = g(x_k) + v_k, \tag{2}$$

where the sensor errors $v_k \sim \mathcal{N}(x, R)$ are assumed to be AWGN. From here, the MAP cost function can be defined. In this optimization problem, the decision variables are the states at each time step during the time horizon of interest $(x_1, \ldots, x_N)$, and measurement histories are known. A nonlinear least squares problem in which the dynamics errors and sensor errors are weighted by the inverse of their noise covariances is then posed:

$$\underset{x_1,\ldots,x_N}{\text{minimize}} \quad \sum_{k=1}^{N-1} (x_{k+1} - f(x_k))^T Q^{-1} (x_{k+1} - f(x_k)) + (y_k - g(x_k))^T R^{-1} (y_k - g(x_k)), \tag{3}$$

which can be rewritten equivalently in the following form:

$$\underset{x_1,\ldots,x_N}{\text{minimize}} \quad \sum_{k=1}^{N-1} \left\| \begin{bmatrix} \sqrt{Q^{-1}}(x_{k+1} - f(x_k)) \\ \sqrt{R^{-1}}(y_k - g(x_k)) \end{bmatrix} \right\|_2^2 \tag{4}$$

From here, the least-squares structure of the problem is evident. To align the formulation here with standard least-squares notation, a residual vector r is defined. The concatenation of all of the decision variables $(x_1, \ldots, x_N)$ will be renamed z

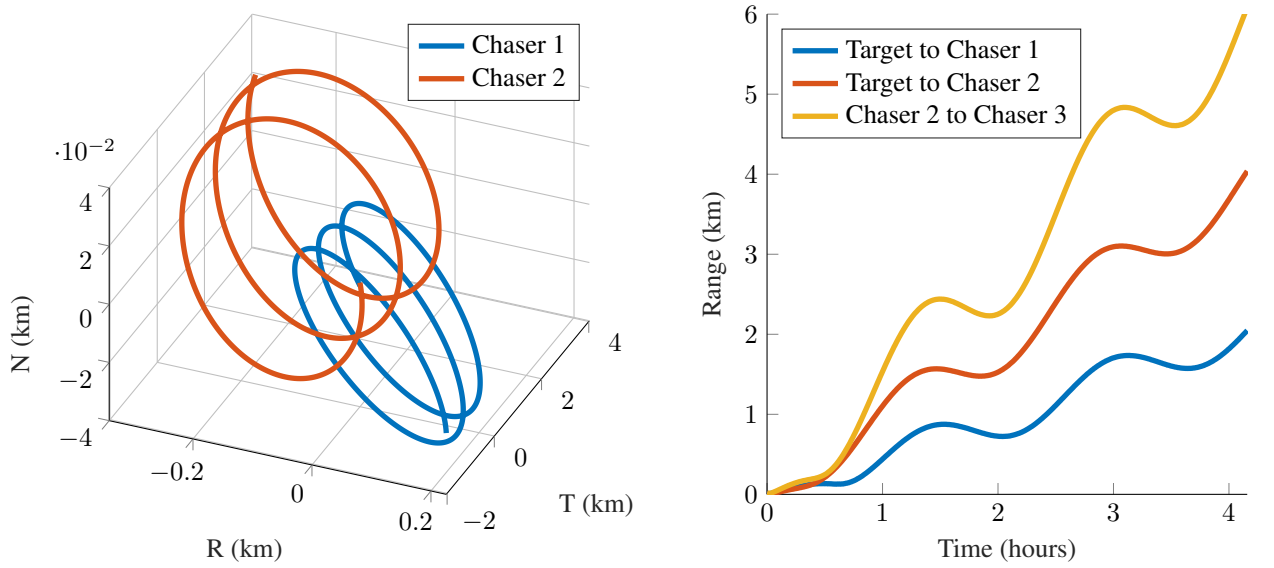

Figure 5. Ground-truth positions of the chaser spacecraft in the RTN frame of the target spacecraft (left), as well as ground-truth ranges between all three spacecraft (right) from a high-fidelity simulation.

to ease the notation in the residual vector:

$$r(z) = \begin{bmatrix} \sqrt{Q^{-1}}(x_{k+1} - f(x_k)) \\ \sqrt{R^{-1}}(y_k - g(x_k)) \\ \vdots \\ \sqrt{Q^{-1}}(x_N - f(x_{N-1}, u_{N-1})) \\ \sqrt{R^{-1}}(y_{N-1} - g(x_{N-1})) \end{bmatrix} \tag{5}$$

The sum of the squares of the elements in this residual vector is the cost function of the original optimization problem. This means the MAP optimization problem can now be re-written in a familiar form for nonlinear least squares problems:

$$\underset{z}{\text{minimize}} \quad \|r(z)\|_2^2 \tag{6}$$

A Levenberg-Marquardt damped least-squares solver as described in Algorithm 1 is then used to minimize the MAP cost function with respect to the state history, thereby recovering the optimal MAP estimates of the orbits of the three spacecraft.

Algorithm 1 Levenberg-Marquardt Damped Least-Squares

input z_0 ▷ initial guess for z
while $\|[\partial r/\partial z]^T r(z)\| >$ tolerance **do** ▷ while the norm of the gradient is above a tolerance
  $J = \partial r/\partial z$ ▷ Jacobian of the residual
  $\Delta z = -(J^T J + \lambda I)^{-1} J^T r(z)$ ▷ solve a regularized linear least squares problem
  $\alpha = \text{linesearch}(z, \Delta z)$ ▷ line search to ensure reduction in cost
  $z \mathrel{+}= \alpha \Delta z$ ▷ update z
end while
return z

This state-estimation technique was validated on simulated data for three spacecraft in low-Earth orbit beginning immediately after deployment. The target spacecraft was at an altitude of 550 km, with an eccentricity of 0.01 and inclination of 45°. To simulate variations in the deployment of the three spacecraft, the two chaser spacecraft were perturbed 10 m in position and .1 m/s in velocity. The orbits of the three spacecraft were propagated using a high-fidelity model that includes high-order gravity, solar radiation pressure, and atmospheric drag. The relative positions of the two chaser spacecraft with respect to the target are shown in Fig. 5.

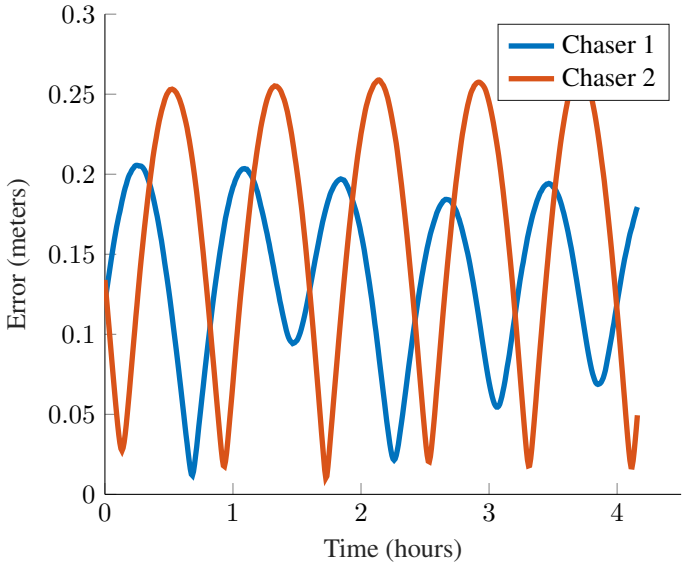

Figure 6. Relative position errors between the chaser spacecraft and the target spacecraft computed using Algorithm 1 in a high-fidelity simulation. Orbits and sensor errors in this simulation are consistent with those of the actual V-R3x mission.

Using the simulated orbits, sensor measurements were generated assuming the GPS on the target spacecraft has a 1-σ accuracy of 10 cm in position, 1 cm/s in velocity, and the relative ranges between the spacecraft have an accuracy of 0.5 m. The resulting errors in the positions of the chaser spacecraft measured in the RTN frame of the target spacecraft are plotted in Fig. 6.

5. TEST CAMPAIGN

5.1. Ridge Testing and High-Altitude Balloon Experiments

Long-range terrestrial testing of crosslink and ranging performance was evaluated for the S-band and UHF radio modules across multiple flight-like spacecraft assemblies. LoRa UHF crosslink was successfully demonstrated at distances greater than 30 km for the following LoRa modulation parameters: frequency=915.6 MHz, Spreading Factor=7, Bandwidth=500 kHz, Coding Rate=4/8.

S-band ranging performance was evaluated across four spacecraft assemblies distributed up to 10 km apart with a direct line of sight. In this test, one unit was chosen arbitrarily as the "leader" to initiate bidirectional ranging between each of the remaining three spacecraft approximately every 5 seconds. During operation, each unit continuously logged GPS position information from its on-board GPS module at a rate of 1 Hz. Testing began once all four units achieved a stable GPS fix, after which the leader spacecraft remained stationary for about 5 minutes before being hand-carried along a 155 meter circular path over about 7 minutes. S-band ranging was conducted using the following LoRa modulation parameters: frequency=2400 MHz, Spreading Factor=10, Bandwidth=800 kHz, Coding Rate=4/4. Due to the nature of this time-of-flight ranging scheme, the SX1280 radios will achieve optimal ranging precision (but shortest maximum distance) using the highest bandwidth setting of 1600 kHz, however, 800 kHz was chosen as a compromise between maximum distance and ranging precision.

Before accurate ranging can be done, the raw ranging results from the S-band radio need to be calibrated to reflect the true range between units. To do this, the distance between GPS measurements x_{gps} was treated as ground truth, and an affine model was fit to the ranging data using linear least squares. More explicitly, the calibrated range measurement $x_{calib.}$ is an affine function of the raw range x_{raw},

$$x_{calib.} = ax_{raw} + b, \tag{7}$$

where a and b are constants. From here, an optimization is formed to solve for the optimal a and b that fit the $x_{calib.}$ to

the GPS distance:

$$\underset{a,\,b}{\text{minimize}} \quad \sum_{k=1}^{N} \left(x_{gps} - (a x_{true} + b)\right)^2 \tag{8}$$

This is a linear least squares problem and the globally optimal affine fit can be solved for in closed form. Using the resulting calibration, post-processed ranging and GPS distance measurements between two terrestrial spacecraft are shown in Fig. 7. In this example, the calibrated ranging was able to track the GPS distance closely, well within the 3-σ accuracy of the GPS positions.

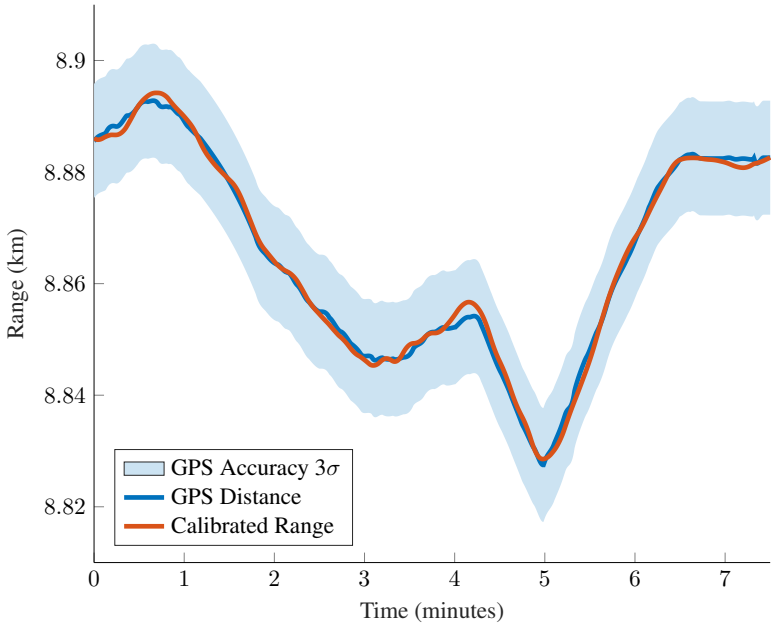

Figure 7. Calibrated ranging measurements overlaid with GPS distance measurements during ridge testing. Two units were placed ≈ 9 km apart and the GPS measurements on each were used to calibrate the S-band ranging. The calibrated ranging signal matches the GPS distance closely, well within the 3-σ accuracy of the GPS position.

A high-altitude balloon experiment was conducted with the intent of further validating RF crosslink and ranging performance. Raven Aerostar was contracted to conduct the balloon experiment on March 12, 2021, which reached an altitude of ≈32 km during its 300 minute, 400 km, journey. Similar to the ridge test, the balloon consisted of one "leader" spacecraft that conducted S-band and UHF activities between four stationary units distributed terrestrially along the flight path. Although on-board GPS and UHF/S-band crosslink activities were successful, a bug in the ranging firmware prevented S-band ranging operations from occurring. Using the same LoRa modulation parameters from the previously discussed ridge testing, the balloon unit achieved UHF and S-band crosslinks, shown in Fig. 9, for the duration of the flight, with the farthest being 384 km.

Figure 8. Launch of the V-R3x high-altitude balloon test on March 12, 2021. A single V-R3x CubeSat is mounted inside the balloon payload seen on the stand in the right of the photograph.

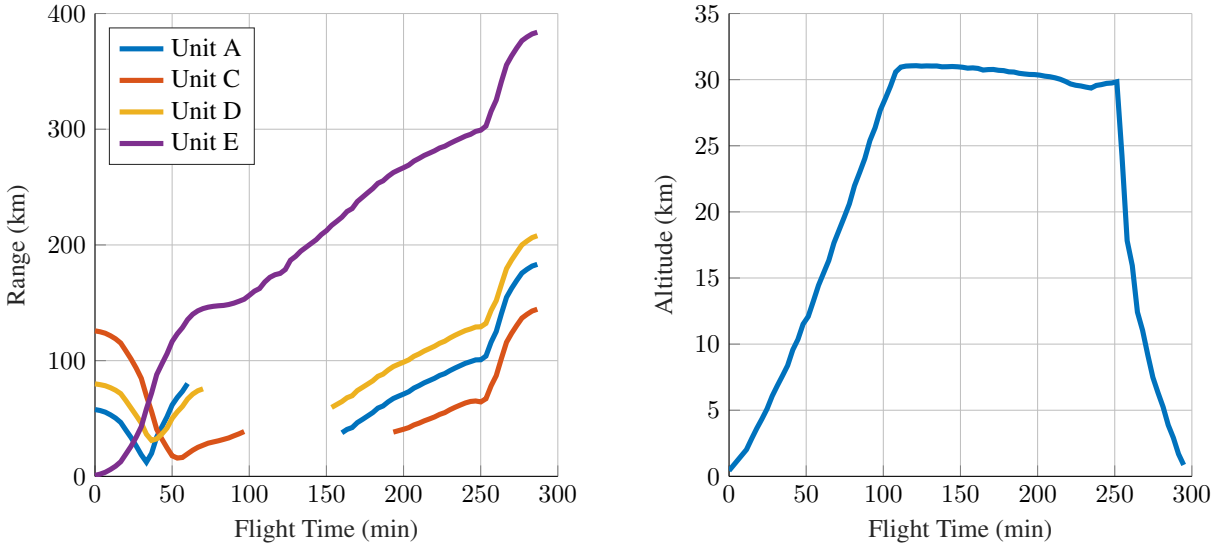

Figure 9. Range measurements collected between the high-altitude balloon V-R3x unit and several ground stations (left) and the altitude profile of the balloon during the test (right).

5.2. On-Orbit Demonstration

Three V-R3x spacecraft launched on the SpaceX Transporter-1 mission on January 24, 2021, and were deployed at an altitude of 525 km into a roughly circular sun-synchronous orbit. Contact was made with the spacecraft shortly after deployment using mobile ground stations located at both Stanford University and Carnegie Mellon University (Fig. 10). Telemetry packets received in the first few hours of the mission indicated that all three spacecraft were experiencing extremely high tumble rates in excess of 30 deg/sec (Fig. 11), as well as generating roughly an order of magnitude less solar power than anticipated. Neither of these initial issues were resolved. As a result, the spacecraft were power-negative throughout their entire mission, and were not able to charge their batteries (Fig. 12). All three spacecraft were commanded into low-power mode on February 13, 2021 to conserve power, after which contact was not re-established.

In spite of these difficulties, the three spacecraft did operate successfully for 20 days, and were able to achieve the majority of the primary mission objectives. Beacon packets were collected at both Stanford and by a network of amateur radio enthusiasts, totaling over 114 packets received in the first 72 hours after deployment. Command and control of the spacecraft was also successfully demonstrated from both Stanford and CMU. The following subsections summarize on-orbit results with respect to each of the primary mission objectives:

5.2.1. Objective 1: S-Band and UHF High-Data-Rate Crosslinks

Full-speed S-band (253 kbps) and UHF (37.5 kbps) high-data-rate crosslinks were successfully conducted between all three satellite nodes numerous times during the gradual separation of the spacecraft after deployment. Each spacecraft's crosslink metrics, such as number of attempts and percentage of dropped packets, was contained within its periodic beacon packets and was, therefore, easily monitored without the necessity of two-way ground station communication. The longest full-speed crosslink distance was achieved at 160 km prior to discontinuing spacecraft operations.

5.2.2. Objective 2: S-Band High-Precision Ranging

Dense ranging datasets were collected between all three satellites alongside real-time GPS positions and velocities. Snippets of the dense ranging datasets were included in the routine beacon transmissions, thereby confirming the successful exchange of time-of-flight LoRa ranging packets. However, due to the power issues encountered during the mission and the need to put the spacecraft into low-power mode, complete datasets were never downlinked from any of the spacecraft and remain trapped in the on-board flash memory.

Figure 10. V-R3x mobile ground station. A low-cost amateur telescope go-to mount is used automatically point a 12 dBi gain 915 MHz helical antenna using standard open-source satellite-tracking software. The antenna is connected to a pair of LoRa radios through a low-noise amplifier for receiving and a 50 W power amplifier for transmitting. The entire setup is portable, can be assembled and disassembled in minutes, and can be powered from a lithium-ion battery pack.

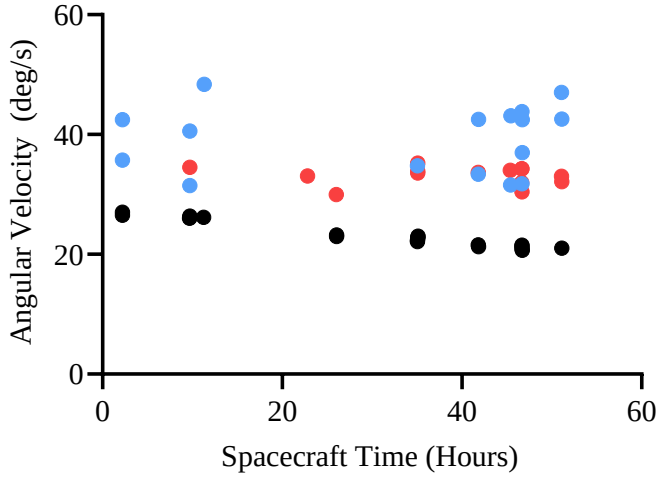

Figure 11. On-orbit gyroscope data illustrating a high tumble rate for each spacecraft as distinguished by VR3X-A (red), VR3X-B (blue), VR3X-C (black).

5.2.3. Objective 3: Relative Navigation

The ranging datasets comprised of precision inter-satellite range measurements, along with GPS position and velocity measurements were to be downlinked from the satellites and processed to determine the relative and absolute positions of all three V-R3x spacecraft. Although the datasets were successfully collected and stored in on-board non-volatile memory, the power generation issues and shortened mission duration prevented the retrieval of a complete dataset from any of the spacecraft. In lieu of complete on-orbit ranging datasets, a series of terrestrial experiments were performed to evaluate hardware performance and limitations.

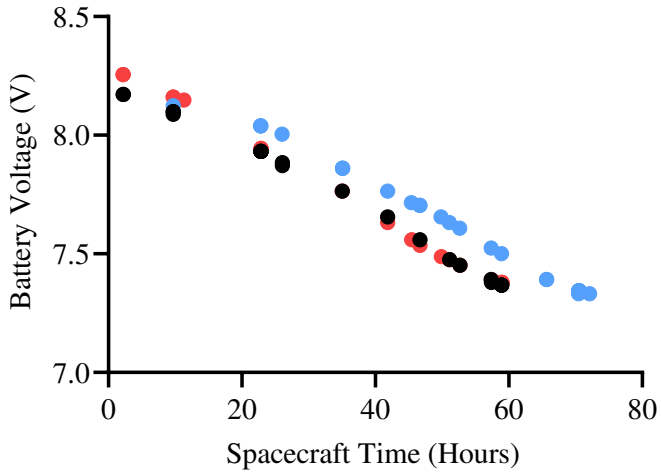

Figure 12. On-orbit battery voltage (8.4 V full, ≈7 V empty) as reported by VR3X-A (red), VR3X-B (blue), VR3X-C (black) spacecraft.

5.2.4. Objective 4: Distributed Sensor Collection

Each spacecraft collected onboard total ionizing-dose (TID) measurements once every 30 seconds with the intent of creating dense temporal and spatial dose-rate datasets to be downlinked and post-processed. It is known from beacon packets that at least seven radiation datasets were collected and stored onboard each spacecraft before ceasing mission operations. Figures 13 and 14 show the snippets of V_{TH} and temperature information that were successfully collected from beacon packets. Due to the nature of the V_{TH} measurements, there is insufficient data to properly estimate cumulative dose, thus the raw voltage shifts are shown, which match the expected TID accumulation for the LEO orbit of the V-R3x mission. The internal temperature measurements, which are achieved by monitoring the voltage across a known bandgap reference, are shown in Fig. 14. A minimum internal temperature of 18.5C and a maximum of 22.4C are reported, which are reasonable values given the sun-synchronous orbit. V-R3x was successful in creating an internal spacecraft thermal environment ideal for microelectronic devices and lithium-polymer battery operation.

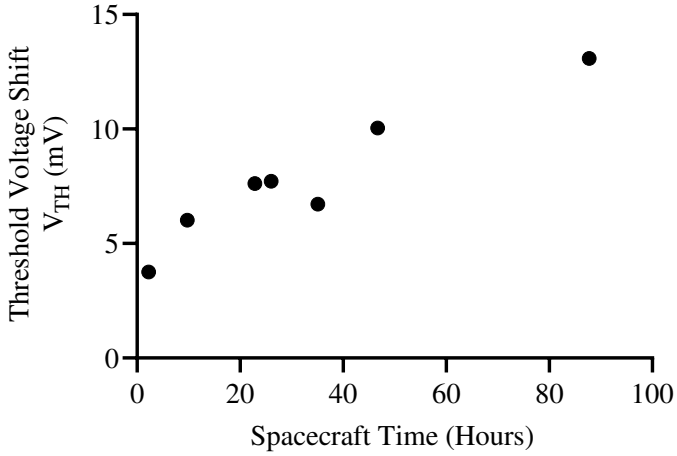

Figure 13. On-orbit raw dosimeter readings (threshold voltage shift) for spacecraft VR3X-C.

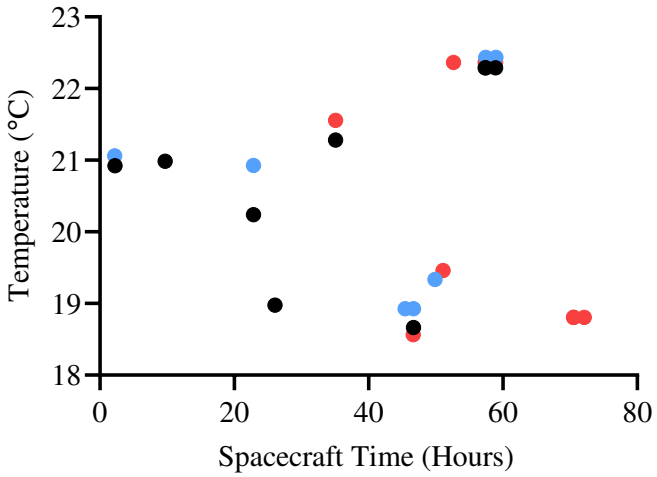

Figure 14. On-orbit internal spacecraft temperature as reported by VR3X-A (red), VR3X-B (blue), VR3X-C (black).

6. LESSONS LEARNED AND CONCLUSIONS

The V-R3x project was successful in moving from initial concept to on-orbit demonstration in under 12 months. In spite of some technical issues encountered on orbit, the mission still managed to achieve many of its primary objectives, including the demonstration of high-data-rate cross links and two-way time-of-flight ranging using low-cost LoRa radios on orbit. Several important lessons were learned throughout the project that we hope are of use to the broader small satellite community:

6.1. Lesson 1: Tumbling Caused by Unconstrained Antenna Deployment

Driven by experiences of the team on prior CubeSat missions in which antenna deployment failures occurred, a decision was made to not secure the UHF dipole antennas on the V-R3x spacecraft with a burn wire and, instead, to insert the spacecraft into the dispenser with the antennas unconstrained such that they would be deployed immediately upon ejection from the dispenser. However, V-R3x experienced another sort of anomaly during deployment: extremely high tumble rates on all three spacecraft. We hypothesize that these high tumble rates were caused by contact between the tape-spring antennas and the walls of the dispenser. The relatively stiff tape springs likely caused large "tip-off" torques on the CubeSats as they exited the dispenser, resulting in the large angular velocities depicted in Fig. 11. We suggest two strategies to mitigate this failure mode in the future: 1) constrain tape-spring antennas with a burn wire to prevent tip-off torques, and 2) implement a controller on the spacecraft, such as the ubiquitous B-dot, that is capable of detumbling the satellite in the event of large initial angular velocities.

6.2. Lesson 2: Effects of Tumbling on Solar Charging

We also hypothesize that tumbling was responsible for the significant decrease in energy harvesting encountered on the V-R3x spacecraft. This is thought to be a result of the V-R3x solar power collection scheme, which utilizes a simple maximum power-point tracking (MPPT) circuit to optimize solar cell energy efficiency. As designed, the MPPT circuit strives to bias the solar array at a fixed percentage (about 75%) of the open-circuit voltage (V_{OC}) as a means of maximizing the array's power production based on the fill factor of its individual cells. During operation, V_{OC} is sampled by briefly disconnecting the load from the solar charging circuit, allowing V_{OC} to rise over the course of about 30 ms, and then adjusting the desired bias set point before reconnecting the cells to resume charging the batteries. Under normal circumstances, the MPPT circuit samples V_{OC} once every 30 seconds, or if a dramatic change in solar input is observed. During tumbling, it is believed the V_{OC} measurement routine is being triggered far more than originally desired, resulting in extended periods of little-to-no battery charging. In addition to the mitigations proposed in Lesson 1, the effects of fast time-varying illumination on spacecraft solar panels should be investigated in pre-flight testing to ensure that energy harvesting electronics do not exhibit hysteretic effects or other failure modes in the presence of tumbling.

The V-R3x team continues to pursue further flight demonstrations for the core technologies documented here. A follow-on mission consisting of four CubeSats, rather than three, is planned for 2023. In addition to addressing the lessons learned during the first V-R3x mission, this follow-on mission will implement distributed navigation algorithms in flight software to run autonomously onboard the spacecraft.

ACKNOWLEDGEMENTS

This work was supported by NASA's Space Technology Mission Directorate (STMD) Small Satellite Technology Program (SSTP) under NASA Grant Numbers 80NSSC18K1673 and 80NSSC21K0466.

REFERENCES

[1] C. Foster, H. Hallam, and J. Mason, "Orbit Determination and Differential-drag Control of Planet Labs Cubesat Constellations," *arXiv:1509.03270 [astro-ph, physics:physics]*, Sep. 2015.

[2] C. Foster, J. Mason, V. Vittaldev, *et al.*, "Constellation Phasing with Differential Drag on Planet Labs Satellites," *Journal of Spacecraft and Rockets*, vol. 55, no. 2, pp. 473–483, Mar. 2018.

[3] B. Lucia, B. Denby, Z. Manchester, H. Desai, E. Ruppel, and A. Colin, "Computational Nanosatellite Constellations: Opportunities and Challenges," *GetMobile: Mobile Computing and Communications*, vol. 25, no. 1, pp. 16–23, Jun. 2021.

[4] S. Engelen, C. J. M. Verhoeven, and M. J. Bentum, "OLFAR: A Radio Telescope Based On Nano-Satellites In Moon Orbit," in *24th AIAA/USU Conference on Small Satellites*, Logan, UT, 2010, p. 7.

[5] S. Wu, W. Chen, Y. Zhang, W. A. Baan, and T. An, "SULFRO: A Swarm of Nano-/Micro-Satellite at SE L2 for Space Ultra-Low Frequency Radio Observatory," in *28th AIAA/USU Conference on Small Satellites*, Logan, UT, 2014.

[6] F. Alibay, J. C. Kasper, T. J. W. Lazio, and T. Neilsen, "Sun radio interferometer space experiment (SunRISE): Tracking particle acceleration and transport in the inner heliosphere," IEEE, Mar. 2017, pp. 1–15.

[7] L. Plice, A. D. Perez, and S. West, "HELIOSWARM: SWARM MISSION DESIGN IN HIGH ALTITUDE ORBIT FOR HELIOPHYSICS," in *AAS/AIAA Astrodynamics Specialist Conference*, Portland, ME, 2019, p. 18.

[8] M. Holliday, A. Ramirez, C. Settle, T. Tatum, D. Senesky, and Z. Manchester, "PyCubed: An Open-Source, Radiation-Tested CubeSat Platform Programmable Entirely in Python," in *AIAA/USU Conference on Small Satellites (SmallSat)*, Aug. 2019, p. 9.

[9] T. Janssen, N. BniLam, M. Aernouts, R. Berkvens, and M. Weyn, "LoRa 2.4 GHz Communication Link and Range," *Sensors*, vol. 20, no. 16, p. 4366, Aug. 2020.

[10] M. Holliday, T. A. Heuser, Z. Manchester, and D. G. Senesky, "Dynamic Biasing for Improved On-Orbit Total-Dose Lifetimes of Commercial Electronic Devices," *IEEE Transactions on Aerospace and Electronic Systems*, pp. 1–1, 2022.

[11] M. V. O'Bryan, K. A. LaBel, S. P. Buchner, *et al.*, "Compendium of Recent Single Event Effects Results for Candidate Spacecraft Electronics for NASA," in *2008 IEEE Radiation Effects Data Workshop*, Jul. 2008, pp. 11–20.

[12] D. J. Cochran, S. P. Buchner, D. Chen, *et al.*, "Total Ionizing Dose and Displacement Damage Compendium of Candidate Spacecraft Electronics for NASA," in *2009 IEEE Radiation Effects Data Workshop*, Jul. 2009, pp. 25–31.

[13] G. R. Allen, "Compendium of Test Results of Single Event Effects Conducted by the Jet Propulsion Laboratory," in *2008 IEEE Radiation Effects Data Workshop*, Jul. 2008, pp. 21–30.

[14] M. Holliday, Z. Manchester, and D. G. Senesky, "On-Orbit Implementation of Discrete Isolation Schemes for Improved Reliability of Serial Communication Buses," *IEEE Transactions on Aerospace and Electronic Systems*, pp. 1–1, 2022.

[15] R. E. Kalman, "A New Approach to Linear Filtering and Prediction Problems," *Journal of Basic Engineering*, vol. 82, no. 1, pp. 35–45, Mar. 1960.

[16] S. Thrun, W. Burgard, and D. Fox, *Probabilistic Robotics*. MIT press, 2005.